

## Partial Ionic Stopping Power and the Energy Expended in Electron Capture and Loss Collisions of Protons in Hydrogen Gas. II\*

M. N. HUBERMAN

*The Enrico Fermi Institute for Nuclear Studies, The University of Chicago, Chicago, Illinois*

(Received March 20, 1962)

The experimental method of Allison, Cuevas, and Garcia-Munoz for measuring atomic partial stopping powers ( $\epsilon_0$ ) has been extended to the determination of the stopping power  $\epsilon_1$  of hydrogen gas for the  $H^+$  component of a hydrogen beam. The protons in a 1-mm diam beam are held in an orbit which is an arc of a circle of 142-cm radius, and are guided to a 1-mm diam exit after a path length of 55.8 cm in  $\sim 50 \mu$  pressure of  $H_2$  gas. The energy of the beam after leaving the stopping cell is measured by electrostatic deflection. No proton thus measured can have experienced a charge-changing collision in the stopping cell. In preliminary experiments protons were simulated by deuterons of twice the energy and  $\epsilon_1$  determined for protons of 55, 75, and 93 keV. Finally, an extended series of runs at 42.8 and 54.2 keV were made on  $\epsilon_1$ , and a similar extended series on  $\epsilon_0$ , with the apparatus arranged as in the work of Allison *et al.* These latter measurements for  $\epsilon_1$ ,  $\epsilon$ , and  $\epsilon_0$  gave  $(6.12 \pm 0.44; 6.36 \pm 0.16; 2.72 \pm 0.16) \times 10^{-15}$  eV cm<sup>2</sup>/atom, and in the same units, for the higher voltage,  $(6.04 \pm 0.39; 6.45 \pm 0.22; 2.91 \pm 0.29)$ .

Since the charge composition of the beam is known from other experiments, the charge-changing collisions may be shown to contribute 34% of the total stopping losses. The sum of the losses in kinetic energy in an electron capture and in its subsequent loss is  $40 \pm 6$  eV at 42.8 keV and  $54 \pm 9$  eV at 54.2 keV, neglecting charge-changing collisions involving  $H^-$ .

### INTRODUCTION

WHILE the retardation by matter of fast charged particles has long been the subject of theoretical study, it is only in recent years that a detailed treatment has been given for the energy region where projectile velocities are of the order of electronic orbital velocities.<sup>1</sup> In this region electron capture and loss play an important role in the stopping process, and a detailed theoretical treatment must take into account not only the various states of ionization of the particle but also the energy loss due to the charge-changing collisions themselves. Recently, Allison, Cuevas, and Garcia-Munoz<sup>2</sup> have introduced an experimental technique which permits the measurement of the atomic partial stopping power  $\epsilon_0$ , i.e., the sum of the losses experienced by  $H^0$  in all types of inelastic collisions in hydrogen gas which do not change its charge. In this paper the method has been extended to the measurement of  $\epsilon_1$ , the analogous ionic partial stopping power for protons, and to a determination of the fraction of the energy lost from a charge-equilibrated beam in collisions resulting in change of charge.

The equation below shows a grouping of the many types of collisions involved, which is suggested by the experimental method. The total stopping power ( $\epsilon$ ) at energies in the region of 50 keV can be described as being the weighted sum of four partial processes; the stopping power for neutral H atoms ( $\epsilon_0$ ), ionized H atoms ( $\epsilon_1$ ), negative H atoms ( $\epsilon_f$ ), and the energy losses due to the collisions involving change of charge. This can

be expressed mathematically as

$$\epsilon = F_{1\infty}\epsilon_1 + F_{0\infty}\epsilon_0 + F_{1\infty}\epsilon_1 + \sum_{if} F_{i\infty}W_{if}\sigma_{if}. \quad (1)$$

Here  $\epsilon$  is the conventional, or total stopping power in eV cm<sup>2</sup>/atom,  $F_{i\infty}$  is the fraction of an equilibrated beam in charge state  $i$ ,  $\sigma_{if}$  is the charge-changing cross section in cm<sup>2</sup> of a collision in which the projectile, originally of charge  $i|e|$ , emerges with charge  $f|e|$ .  $W_{if}$  is the energy in electron volts lost in the  $i \rightarrow f$  charge-changing collision.

We have performed our experiments with a hydrogen beam passing through molecular hydrogen gas where the results can be roughly compared with theoretical predictions for beams in atomic hydrogen gas.

### APPARATUS

The conventional experimental arrangement for measuring  $\epsilon$ , and the measurement of  $\epsilon_0$  by placing the stopping cell in a transverse magnetic field were almost identical with that of the preceding paper and will not be described here. The arrangement for measuring  $\epsilon_1$  is shown in Fig. 1. The stopping chamber is placed in a magnetic field which is used to hold the protonic constituent of the beam in an orbit of radius of curvature 142 cm, guiding it to a small exit aperture and resulting in a deflection of  $21^\circ$ .  $\epsilon_1$  may be computed by a subsequent electrostatic analysis of the decrement in energy of the protons caused by admission of the gas.

Two beam sources were used during the measurements. In the first group of measurements a Cockcroft-Walton accelerator provided a deuteron beam, which was used at 186, 150, and 110 kV, to simulate protons of half the corresponding kinetic energies. After several determinations showed that measurements of  $\epsilon_1$  were feasible, it was decided to use a smaller accelerator and study intensively actual proton beams in the kinetic

\* This work was supported in part by the U. S. Atomic Energy Commission.

<sup>1</sup> A. Dalgarno and G. W. Griffling, Proc. Roy. Soc. (London) **A232**, 423 (1955).

<sup>2</sup> S. K. Allison, J. Cuevas, and M. Garcia-Munoz, preceding paper [Phys. Rev. **127**, 792 (1962)], hereinafter referred to as I.

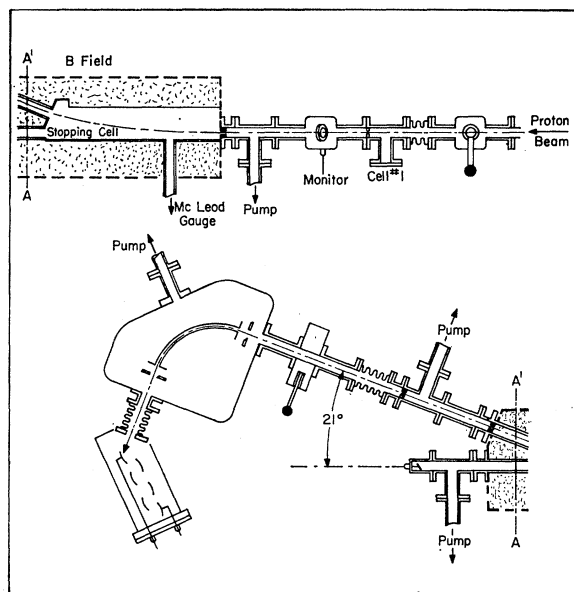


FIG. 1. Apparatus for the measurement of ionic partial stopping power ( $\epsilon_1$ ). Equilibrator and stripper cells No. 1 and No. 3 are in place but not in use; they are needed when the apparatus is rearranged for an  $\epsilon_0$  measurement on the undeviated beam. The length of the curved path in the magnetic field is 55.8 cm.

energy region from 40 to 50 keV, where neutral atoms comprise 50% of the equilibrated beam in hydrogen. Sets of measurements of  $\epsilon$ ,  $\epsilon_1$ , and  $\epsilon_0$  were made in this limited energy range; at least seven acceptable determinations were averaged to establish each value. At the lower energies, the source of the beam was an electrostatic accelerator powered by a 0–50 kV dc stabilized power supply. A rf ion source<sup>3</sup> supplied unanalyzed beam intensities of the order of 50  $\mu$ A from which a  $10^\circ$  deflection magnet sorted out the proton beam. In measurements of  $\epsilon_1$ , where, as in the measurements of  $\epsilon_0$  described in I, there are losses in intensity corresponding to factors of  $10^{-7}$ , the protons remaining in orbit are subsequently detected by an Allen secondary electron multiplier<sup>4</sup> placed behind the exit slit of a 15-cm radius cylindrical electrostatic energy analyzer. The electrostatic analyzer is operated with entrance and exit slit widths of 0.05 cm, which allows a full width at half maximum of 1/600 for a monoenergetic source.<sup>5</sup>

The determination of  $\epsilon_1$  is somewhat simpler than that of  $\epsilon_0$ , in that it is not necessary to charge equilibrate the proton beam before it enters the stopping cell, or to strip it before electrostatic analysis of its energy. Thus, the situation is more favorable as regards intensity losses and there are not so many small apertures to align. On the other hand, the initial setting up of the

<sup>3</sup> S. K. Allison and E. Norbeck, Jr., *Rev. Sci. Instr.* **27**, 285 (1956).

<sup>4</sup> Leticia del Rosario, *Phys. Rev.* **74**, 304 (1948); also J. S. Allen, *ibid.* **55**, 336, 966 (1939).

<sup>5</sup> S. K. Allison, S. P. Frankel, T. A. Hall, J. H. Montague, A. H. Morrish, and S. D. Warshaw, *Rev. Sci. Instr.* **20**, 735 (1949).

experiment was more difficult, since the beam path included a curved orbit, and the apertures could not be aligned visually.

The length of path in the orbit in  $H_2$  gas was 55.8 cm. As in the preceding paper, windows could not be used to contain the gas in the chamber because of the low beam energy. Therefore, 0.09-cm diam tapered holes at the entrance and exit to the chamber allowed us to maintain differential pressure ratios of 1:80 outside the chamber, in addition to providing a rigorous beam geometry for the elimination of protons undergoing electron capture or nuclear scattering.

Since energy losses of the order of 1% of the total beam energy must be measured, a galvanometer and resistor stack (Fig. 2) were used to monitor voltage fluctuations at the probe of the ion source. With the high voltage set at approximately the desired value, the galvanometer is balanced so that no current flows through it. Any subsequent changes in high voltage result in a change in current in the resistor stack and a deflection of the galvanometer because of its low impedance. With this arrangement, fluctuations of one part in  $10^4$  could be detected and corrected for, in interpreting the data.

The inner and outer plates of the electrostatic analyzer were symmetrically charged by precision regulated dc supplies. In addition, the negative supply for the inner plate had a floating ground whose potential could be varied through  $\pm 250$  V by means of a battery and voltage divider combination. Energy losses were measured by the variation in this potential needed to bring the beam back through the analyzer. Changes in potential were read from a Simpson meter which had been calibrated against a precision potentiometer. It is interesting to note at this point that, for the nonrelativistic case, if one measures energy changes on an electrostatic analyzer by varying the potential of one of the plates by an amount  $\Delta V$ , the corresponding energy change is  $\Delta E = k\Delta V$ , where  $k$  is the analyzer constant for completely asymmetric charging of the analyzer (as if the voltage on the other plate were zero) regardless of the actual over-all symmetry of the charge on the analyzer. This can be shown to follow from physical considera-

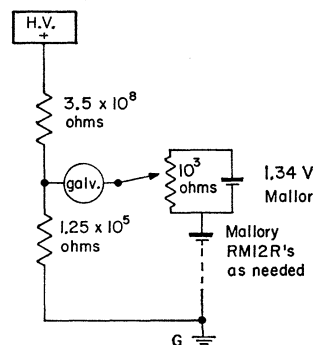


FIG. 2. Monitor circuit for observing deviations of the order of 0.01% in the accelerator high voltage.

tions or from differentiation of the nonrelativistic form of the analyzer equation [Eq. (41), of reference 5].

Absolute pressures in the stopping cell, and in the drift tubes just outside it were read on a McLeod gauge. An alphasatron gauge served as a continuous reading monitor of the stopping cell. The stopping gas was electrolytic hydrogen further purified by passage through a "Deoxo" catalytic purifier followed by a liquid nitrogen trap. A needle valve regulated the rate of flow into the chamber.

Other precautions and equipment used have already been described in I.

#### PROCEDURE OF MEASUREMENT

The partial and total stopping powers were determined from a series of runs in which the stopping chamber was alternately evacuated and brought to the desired pressure of  $H_2$  gas. Stopping pressures ranged from 15 to 50  $\mu$ . The evacuation of the chamber could be expedited by opening a valve leading to a liquid nitrogen trapped mercury vapor pump.

Since beam intensities at the detector were of the order of  $10^{-10}$  A with the stopping chamber evacuated, it was possible when making  $\epsilon$  determinations to measure currents directly, using a vibrating reed electrometer to detect the current collected on the first dynode of the secondary electron detector. However, for  $\epsilon_0$  and  $\epsilon_1$  determinations with gas in the stopping chamber, charge changing collisions and elastic scattering reduced the beam intensity to approximately 100 particles per sec. In this case, individual counts from the secondary electron multiplier were recorded on a scaler for 15-sec intervals. The gas pressure for any given run was chosen to be the maximum compatible with an observable counting rate.

The measured energy spread of the initial beam (Fig. 3) was of the order of 500 eV, and had a double-peaked structure. This is due to three effects; accelerator ripple (0.1%), finite window of the electrostatic analyzer (0.2%), and the energy distribution of the protons produced by the ion source. The greater part of the energy spread and also the doubled peak is most probably due to the latter effect, which is the result of collisions creating ions in the cathode fall region<sup>6</sup> of the source. This effect can be expected to produce spreads greater than 500 eV, but they are not observed because of the momentum resolution of the  $10^\circ$  sorting magnet in combination with the severe geometry of the experiment. The double-peaked structure is washed out by energy straggling when gas is introduced into the stopping chamber. Relatively large straggling is to be expected for the small energy losses encountered in this experiment since these losses correspond to an average of only 20 to 50 ionizing collisions per projectile. For a more quantitative estimate a calculation based on

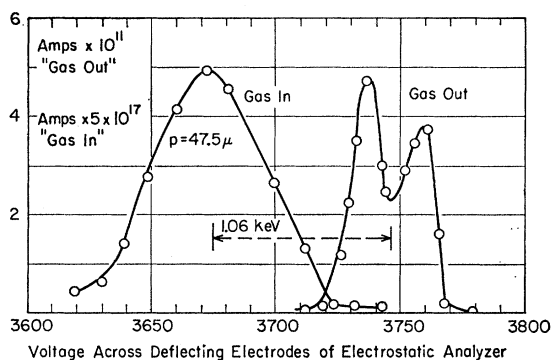


FIG. 3. Energy vs intensity profiles in a typical  $\epsilon_1$  measurement. The double-peaked energy profile in "gas out" is typical of the ion source and accelerator; the structure is washed out by straggling in the "gas-in" curve. Kinetic energies in keV may be obtained by multiplying abscissas by 0.148.

Bethe's straggling formula<sup>7</sup> gives a root mean square energy fluctuation of 30% for a 500-eV energy loss in an  $\epsilon_1$  measurement. However, since this fluctuation is greater than the maximum energy transferable in one proton-electron collision, and since our geometry excludes nuclear collision, we can expect the straggling to be approximately Gaussian.<sup>8</sup>

An important problem in interpreting the data is in defining an energy shift derivable from a small shift in a large distribution which changed shape in the course of the shift. The method adopted was to measure the average of the energy shift of the leading and final edges of the energy distribution. The significance of this can be seen from what would happen to a hypothetical initially rectangular energy distribution. The only well-defined energies we can work with in such a case are those of the leading edge, trailing edge, and the axis of symmetry. Actually the third of these can only be defined in terms of the first two. Straggling will cause an apparent increase in the retardation of the low-energy edge and a decrease for the high-energy edge. However, since the straggling is approximately Gaussian, these effects are canceled out by taking the average of the stopping for the two edges, or in other words, by measuring the shift in the axis of symmetry. This procedure was adopted for the actual energy distributions encountered in this experiment.

In the measurement of  $\epsilon_1$ , a correction had to be made for the rapid variation with energy of  $\sigma_{10}$ , the cross section for electron capture. This cross section changed by several percent within the energy spread of the beam. For a "gas-in" run, the resultant energy-dependent attenuation distorted the original energy distribution. The attenuation is given by

$$I(E) = I_0 e^{-N\sigma_{10}(E)}, \quad (2)$$

<sup>7</sup> M. S. Livingston and H. A. Bethe, *Revs. Modern Phys.* **9**, 245 (1937) [Eq. (788)].

<sup>8</sup> N. Bohr, *Kgl. Danske Videnskab. Selskab, Mat.-fys. Medd.* **18**, No. 8 par. 2.4 (1948).

<sup>6</sup> R. Holz and H. Löb, *Z. Naturforsch.* **13a**, 602 (1958).

where  $N$  is the number of target atoms per  $\text{cm}^2$  and  $I$  is the original intensity. To first order, the variation of  $\sigma_{10}(E)$  is given by

$$\sigma_{10}(E+\Delta E) = \sigma_{10}(E) + \Delta E(d\sigma_{10}/dE)E.$$

Thus,

$$I(E+\Delta E) = I(E)e^{-N(d\sigma_{10}/dE)E\Delta E}. \quad (3)$$

If we neglect the dependence of  $I_0$  on  $E$ ,  $d\sigma_{10}/dE$  can be obtained by differentiating the expression for  $\sigma_{10}$  given by Jackson and Schiff.<sup>9</sup> At 50 keV we find  $d\sigma_{10}/dE = 0.41 \times 10^{-17} \text{ cm}^2/\text{keV}$ . Examination of our data showed that the experimental values of  $\epsilon_1$  had to be raised by 2% to correct for this effect.

For each run on  $\epsilon_0$ , the absolute pressures in both the stopping chamber and outer cells were read with a McLeod gauge. Frequently, the stopping chamber pressure was read twice, once at the beginning and once at the end of a run to ensure that no pressure variations occurred during the run. The stopping chamber was also continuously monitored with an alphasatron vacuum gauge. Temperatures were read from a mercury thermometer placed flush against the outer wall of the stopping chamber.

The procedure on a given run was first to record beam intensity vs analyzer voltage at 10-V intervals, then return to the beginning and record at in-between points. In this way a smooth curve indicates that beam conditions had remained constant during the run. A further check was to compare "gas-out" runs taken immediately preceding and following a "gas-in" run. The variations were never more than would be expected from normal measuring uncertainties.

### ERRORS

Meter reading uncertainties contributed an error of  $\pm 0.1 \times 10^{-15} \text{ eV cm}^2/\text{atom}$  in the stopping powers. Uncertainty in locating the axis of symmetry, due to slight asymmetries in the energy distribution and also because of counting statistics, contributed an error of  $\pm 0.2 \times 10^{-15} \text{ eV cm}^2/\text{atom}$ . Pressure variations during a run were less than 1%.

TABLE I. Results.

| Quantity measured | Kinetic energy <sup>a</sup> (keV) | Experimental results | Previous experimental measurements | Theory (for H <sup>0</sup> gas) |
|-------------------|-----------------------------------|----------------------|------------------------------------|---------------------------------|
| $\epsilon$        | 42.2                              | 6.36±0.16            | 6.29±0.21                          | 6.80                            |
|                   | 53.7                              | 6.45±0.22            | 6.44±0.22                          | 7.15                            |
| $\epsilon_0$      | 41.8                              | 2.91±0.29            | ...                                | 2.18                            |
|                   | 52.1                              | 2.72±0.16            | ...                                | 2.24                            |
| $\epsilon_1$      | 44.8                              | 6.12±0.44            | ...                                | 7.23                            |
|                   | 55.0 <sup>b</sup>                 | 5.70±0.6             | ...                                | 6.94                            |
|                   | 56.7                              | 6.04±0.39            | ...                                | 6.84                            |
|                   | 75 <sup>b</sup>                   | 5.70±0.55            | ...                                | 6.21                            |
|                   | 93 <sup>b</sup>                   | 5.07±0.5             | ...                                | 5.68                            |

<sup>a</sup> Energies are averaged over several runs within an interval of  $\sim 1 \text{ keV}$ .  
<sup>b</sup> Deuteron runs.

<sup>9</sup> J. D. Jackson and H. Schiff, Phys. Rev. **89**, 359 (1953).

TABLE II. Classification of collisions.

| Theoretical classification<br>Dalgarno and Griffing  | Experimental classification |              |                                       |
|--|-----------------------------|--------------|---------------------------------------|
|  | $\epsilon_0$                | $\epsilon_1$ | $\sum F_{i\infty} W_{if} \sigma_{fi}$ |
| A. Ionization by H <sup>+</sup> impact, H <sup>0</sup> (H <sup>+</sup> ; H <sup>+</sup> ,e)H <sup>+</sup>  |                             |              | A                                     |
| B. Excitation by H <sup>+</sup> impact, H <sup>0</sup> (H <sup>+</sup> ; H <sup>*</sup> )H <sup>+</sup>  |                             |              | B                                     |
| C. Capture and excitation by H <sup>+</sup> impact, H <sup>0</sup> (H <sup>+</sup> ; H <sup>+</sup> )H <sup>*</sup>  |                             |              | $C \times F_{1\infty}$                |
| D. H <sup>+</sup> momentum loss in capture, H <sup>0</sup> (H <sup>+</sup> ; H <sup>+</sup> )H <sup>0</sup>  |                             |              | $D \times F_{1\infty}$                |
| E. Single ionization by H <sup>0</sup> impact, H <sup>0</sup> (H <sup>0</sup> ; H <sup>+</sup> ,e)H <sup>0</sup> or H <sup>0</sup> (H <sup>0</sup> ; H <sup>0</sup> ,e)H <sup>+</sup>  | $\frac{1}{2}E$              |              | $\frac{1}{2}E \times F_{0\infty}$     |
| F. Double ionization by H <sup>0</sup> impact, H <sup>0</sup> (H <sup>0</sup> ; H <sup>+</sup> ,2e)H <sup>+</sup>  |                             |              | $F \times F_{0\infty}$                |
| G. Single excitation by H <sup>0</sup> impact, H <sup>0</sup> (H <sup>0</sup> ; H <sup>*</sup> )H <sup>0</sup> or H <sup>0</sup> (H <sup>0</sup> ; H <sup>0</sup> )H <sup>*</sup>      |                             | G            |                                       |
| H. Double excitation by H <sup>0</sup> impact, H <sup>0</sup> (H <sup>0</sup> ; H <sup>*</sup> )H <sup>*</sup>   |                             | H            |                                       |
| I. Ionization and excitation by H <sup>0</sup> impact, H <sup>0</sup> (H <sup>0</sup> ; H <sup>+</sup> ,e)H <sup>*</sup> or H <sup>0</sup> ; H <sup>*</sup> ,e)H <sup>+</sup>          | $\frac{1}{2}I$              |              | $\frac{1}{2}I \times F_{1\infty}$     |
| J. Capture and excitation by H <sup>0</sup> impact, H <sup>0</sup> (H <sup>0</sup> ; H <sup>-</sup> )H <sup>+</sup> or H <sup>0</sup> (H <sup>0</sup> ; H <sup>+</sup> )H <sup>-</sup> |                             |              | $J \times F_{0\infty}$                |
| K. H <sup>-</sup> loss on impact, H <sup>0</sup> (H <sup>-</sup> ; H <sup>0</sup> ,e)H <sup>0</sup>  |                             |              | $K \times F_{T\infty}$                |

The window width of the electrostatic analyzer was equivalent to a variation in stopping power of  $0.6 \times 10^{-15} \text{ eV cm}^2/\text{atom}$ . Since we should be able to detect energy variations of the order of 1/10 of this amount, the resulting uncertainty is  $\pm 0.06 \times 10^{-15} \text{ eV cm}^2/\text{atom}$ .

Another possible source of error in an  $\epsilon_1$  experiment can be due to neutral atoms being formed near enough to the exit of the stopping cell so that their deviation from the main beam is not sufficient to prevent their reaching the energy analyzer. The angle of acceptance of the analyzer is approximately (beam width + analyzer entrance slit width)/(path length to analyzer) = 0.15/62.5 or 0.0024 rad. The curvature of the orbit is 0.007 rad/cm. Therefore, the neutralization would have to take place in the last 1/3 cm of the orbit. At a pressure of 50  $\mu$  the mean free path for electron capture is 3.6 cm. Thus, less than 1/10 of the beam is neutralized in traversing this path. Since 1/3 cm is 0.6% of the total stopping path this effect should contribute less than 0.06% error.

The most difficult error to estimate is that due to nonrandom beam fluctuations. In order to minimize this effect approximately ten independent measurements of each stopping power were made for each energy. This enabled us to calculate a standard deviation for these measurements. To allow for nonrandomness the errors quoted in Table I are 0.67 standard deviation rather than the usual probable error associated with the accuracy attainable in locating the mean of a standard distribution.

### RESULTS AND DISCUSSION

The experimental results on  $\epsilon_0$ ,  $\epsilon_1$ , and  $\epsilon$  (in  $10^{-15} \text{ eV cm}^2/\text{atom}$ ) are included in Table I.

Apart from the deuteron runs, which, as explained before, were in the nature of preliminary determinations, all values in Table I are the average of at least seven independent measurements. The errors quoted in Table I reflect not only the uncertainty of our measurements, but also the 5% accuracy claimed for  $F_{1\infty}$  and  $F_{0\infty}$ .<sup>10</sup> The values of the total stopping power  $\epsilon$  are in excellent agreement with previous experiments<sup>11</sup> and serve to check our procedures. The theoretical results are those of Dalgarno and Griffing<sup>1</sup> (DG) for stopping in atomic hydrogen.

The results listed in Table I, when inserted into Eq. (1), enable us to calculate experimental values of  $\sum F_{i\infty}\sigma_{if}W_{if}$ , the energy loss due to charge-changing collisions. This is possible because  $F_{0\infty}$  and  $F_{1\infty}$  are known experimentally from other work and  $F_{i\infty}$  has been measured from 3 to 30 keV.<sup>10</sup>  $F_{i\infty}$  reaches a maximum of 0.020 at about 15 keV, and by 30 keV it has decreased to 0.014. Since  $\epsilon_I$  must be of the same order as  $\epsilon_1$ , the term  $F_{i\infty}\epsilon_I$  must at least two orders of magnitude lower than  $F_{1\infty}\epsilon_1$ . Thus, although  $\epsilon_I$  was not measured, we can compute the contribution of charge-changing events to the stopping power by solving Eq. (1) for  $\sum$ , using only our  $\epsilon_0$ ,  $\epsilon_1$ , and  $\epsilon$  data. These results are shown in Fig. 4. This method of measuring  $\sum$  has a large error because it involves the difference between two quantities of equal magnitude, each with its own error.

It is interesting to note that charge-changing events account for a large fraction (1/3) of the total stopping power (See Fig. 4.) This is in part due to our choice of an energy near the maximum of the cross section for the charge-changing cycle  $H^+ \rightarrow H^0 \rightarrow H^+$ . This cross sec-

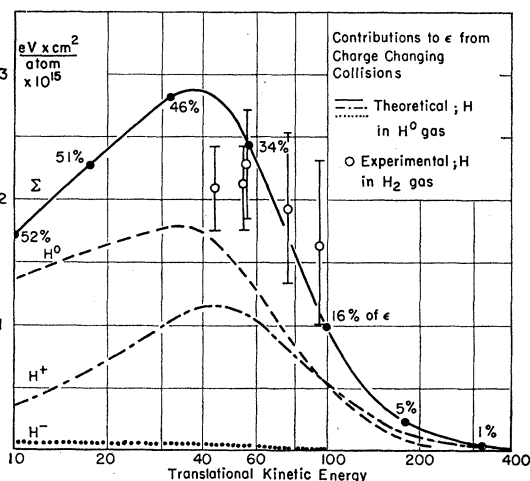


FIG. 4. Theoretical calculations and experimental measurements of contributions to the total stopping power from charge-changing collisions. Percentages shown refer to the total stopping power  $\epsilon$ , from all causes.

<sup>10</sup> P. M. Stier and C. F. Barnett, Phys. Rev. **103**, 896 (1956) as compiled by S. K. Allison, Revs. Modern Phys. **30**, 1137 (1958).

<sup>11</sup> W. Whaling, *Handbuch der Physik* (Springer-Verlag, Berlin, 1958), Vol. 34, p. 193.

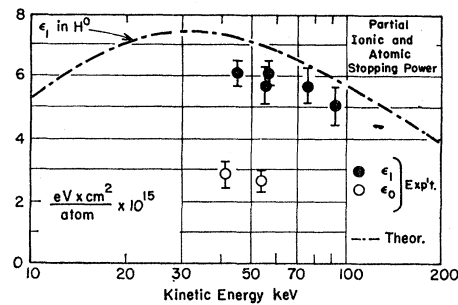


FIG. 5. Partial ionic ( $\epsilon_1$ ) and atomic ( $\epsilon_0$ ) stopping powers compared to the theoretical calculation of  $\epsilon_1$  in atomic hydrogen gas.

tion,  $\sigma_c$ , obtained from the sum of the mean free paths for electron capture and subsequent loss, is equal to  $\sigma_{10}\sigma_{01}/(\sigma_{10}+\sigma_{01})$ , where  $\sigma_{if}$  is the cross section for the process  $H^i \rightarrow H^f$ . It is only when the cycle cross section is large that it is possible for the projectile to continually undergo charge-changing collisions rather than spend most of its time in one charge state.

Turning now to the theory, the stopping processes are grouped by DG into contributions from various possible inelastic events occurring in collisions of  $H^-$ ,  $H^0$ , and  $H^+$  projectiles in  $H^0$  gas. The experiments reported here on  $\epsilon_0$  and  $\epsilon_1$  measure only the charge-invariant contributions from  $H^0$  and  $H^+$  collisions. Fortunately, the DG calculations are further subgrouped in such a manner that they can be rearranged to yield the quantities we have measured. This is done in Table II. The first column lists DG's classifications which are more fully explained in their paper. The subsequent columns show the regrouping necessary for comparison with our experiment.

The agreement with theory is as good as can be expected. In I, it was shown that the theory predicts, in the 40–50 keV energy range, values of  $\epsilon_0$  which are some 20% lower than those observed, but the experiments themselves have an estimated uncertainty as high as  $\pm 10\%$ . Also, as noted in I, the theory predicts too high a value of the total stopping powers for these energies. We find a similar disagreement for  $\epsilon_1$ , as shown in Table I and Fig. 5.

The differences in  $\epsilon_1$  are in the same direction as the deviations from the theory found below 60 keV in recent measurements of the gross-ionization cross section for  $H^+$  and  $H^0$  in molecular hydrogen.<sup>12</sup> At energies above 60 keV, ionization cross sections agree with theory. However, Bates<sup>13</sup> has shown that at energies below several hundred keV, failure to consider distortion in the Born approximation calculations of Bates and Griffing<sup>14</sup> for excitation of hydrogen by protons to the  $2s$  state leads to overestimates of the cross section for this reaction. Therefore, the disagreement for  $\epsilon_1$  above

<sup>12</sup> Fred Schwirzke, Z. Physik **157**, 510 (1960).

<sup>13</sup> D. R. Bates, Proc. Phys. Soc. (London) **73**, 227 (1959).

<sup>14</sup> D. R. Bates and G. W. Griffing, Proc. Phys. Soc. (London) **A66**, 961 (1953).

TABLE III. Sum of the energies lost in the capture and subsequent loss of an electron.

| Kinetic energy of translation (keV) | $(W_{01}+W_{10})$ (eV) |
|-------------------------------------|------------------------|
| 42.8                                | 40±6                   |
| 54.2                                | 54±9                   |
| 55                                  | 61±12                  |
| 75                                  | 86±22                  |
| 93                                  | 118±23                 |

60 keV may be due to the theory predicting too high an excitation loss.

The experimental values of the sum of the contribution to the stopping power from charge-changing collisions are compared in Fig. 4 with the sum of the items in the fourth column of Table II, as calculated by DG. At energies above 50 keV, the agreement seems satisfactory; the experimental errors rise rapidly with energy because the information sought must be obtained by subtraction of essentially the term  $\epsilon_1 F_{1\infty}$  from  $\epsilon$ , and these become more and more the same. The result at 42.8 keV seems to indicate a different behavior of the curve for  $H^+$  in  $H_2$  than that calculated for  $H^+$  in  $H^0$ . The difference may be due to the resonant nature of the reaction  $H^0(H^+,H^0)H^+$  which is true charge exchange and enhances the cross section for this reaction in the atomic hydrogen cases. There is no such resonance in  $H_2(H^+,H^0)H_2^+$ .

The expansion of the summation which represents the charge-changing collisions in the right-hand member of Eq. (1) is

$$\sum F_{i\infty} W_{ij} \sigma_{ij} = F_{1\infty} W_{10} \sigma_{10} + F_{0\infty} (W_{01} \sigma_{01} + W_{01} \sigma_{01}) + F_{1\infty} W_{10} \sigma_{10}. \quad (4)$$

The experiments reported here, in themselves, do not permit a separate evaluation of the various quantities, but it is reasonable to trust the theory as to the relative importance of the two terms involving  $H^-$ . The theoretical contributions involving  $H^-$  must be less than item  $J \times F_{0\infty}$  plus item  $K \times F_{1\infty}$ , since item  $J$  includes the additional process  $H^0(H^0, H^+)H^-$ . Calculations then show that  $F_{1\infty} W_{1\infty} \sigma_{10} + F_{0\infty} W_{01} \sigma_{01}$  contributes less than 2.3% to the theoretical total stopping power. At higher energies, this contribution becomes even less significant.

Thus, to the accuracy of the present work, theory indicated reliably that in our energy range the effective value of the sum of Eq. (1) is

$$F_{0\infty} W_{01} \sigma_{01} + F_{1\infty} W_{10} \sigma_{10} = \sigma_c (W_{01} + W_{10}). \quad (5)$$

$(W_{01} + W_{10})$  is the total energy lost in electron volts in the two charge-changing events involved in the  $H^+ \rightleftharpoons H^0$  cycle. The numerical values are given in Table III.

A significant part of the increase of  $(W_{10} + W_{10})$  with energy as seen in Table III is the increasing momentum which must be imparted to the electron in the target atom to capture it into the moving set of coordinates appropriate to the projectile.

Finally, there is the question of the validity of applying atomic theories to processes in molecular hydrogen. The Bragg rule for the addition of atomic stopping powers to obtain molecular stopping powers has been shown to fail for protons of energy less than 150 keV incident on the compounds  $NH_3$  and  $H_2O$ .<sup>1,15</sup> Even apparent successes of the atomic theory are suspect. Tuan and Gerjuoy<sup>16</sup> have shown that the ability of atomic theories to predict  $\sigma_{10}$  is due to a fortuitous cancellation of the matrix elements which appear in an exact treatment of the problem for energies less than 400 keV.

Because of the above-mentioned reasons we feel that the real importance of these experiments will lie in their comparison with future theories for stopping in molecular hydrogen. Recent advances in theoretical, experimental, and computer techniques should make at least a semiempirical theory possible.

#### ACKNOWLEDGMENTS

The author wishes to thank Professor Samuel K. Allison for suggesting this problem, for extending the facilities of his laboratory, and for his constant advice and encouragement without which this work would not have been possible. Grateful acknowledgment is also made to Dr. Jesus Cuevas and Dr. Moises Garcia-Munoz for many helpful discussions and for assistance in obtaining the data. Thanks are due to John Erwood for maintaining the equipment.

<sup>15</sup> H. K. Reynolds, D. N. F. Dunbar, W. A. Wenzel, and W. Whaling, Phys. Rev. **92**, 742 (1953).

<sup>16</sup> T. F. Tuan and E. Gerjuoy, Phys. Rev. **117**, 756 (1960).